

# Light extraction efficiency of GaN-based LED with pyramid texture by using ray path analysis

Jui-Wen Pan<sup>1,2,3,\*</sup> and Chia-Shen Wang<sup>4</sup>

<sup>1</sup>*Institute of Photonic Systems, National Chiao Tung University, Tainan City 71150, Taiwan*

<sup>2</sup>*Biomedical Electronics Translational Research Center, National Chiao Tung University, Hsin-Chu City 30010, Taiwan*

<sup>3</sup>*Department of Medical Research, Chi Mei Medical Center, Tainan 71004, Taiwan*

<sup>4</sup>*Institute of Imaging and Biomedical Photonics, National Chiao Tung University, Tainan City 71150, Taiwan*

*\*juuwenpan@gmail.com*

**Abstract:** We study three different gallium-nitride (GaN) based light emitting diode (LED) cases based on the different locations of the pyramid textures. In case 1, the pyramid texture is located on the sapphire top surface, in case 2, the pyramid texture is located on the P-GaN top surface, while in case 3, the pyramid texture is located on both the sapphire and P-GaN top surfaces. We study the relationship between the light extraction efficiency (LEE) and angle of slant of the pyramid texture. The optimization of total LEE was highest for case 3 among the three cases. Moreover, the seven escape paths along which most of the escaped photon flux propagated were selected in a simulation of the LEDs. The seven escape paths were used to estimate the slant angle for the optimization of LEE and to precisely analyze the photon escape path.

©2012 Optical Society of America

**OCIS codes:** (230.3670) Light-emitting diodes; (220.4000) Microstructure fabrication.

---

## References and links

1. J. W. Pan and C. W. Fan, "High luminance hybrid light guide plate for backlight module application," *Opt. Express* **19**(21), 20079–20087 (2011).
2. E. F. Schubert, *Light-Emitting Diodes*, 2nd ed. (Cambridge University Press, 2006.) pp. 91–93.
3. Y. K. Ee, P. Kumnorkaew, R. A. Arif, H. Tong, J. F. Gilchrist, and N. Tansu, "Light extraction efficiency enhancement of InGaN quantum wells light-emitting diodes with polydimethylsiloxane concave microstructures," *Opt. Express* **17**(16), 13747–13757 (2009).
4. H. Ichikawa and T. Baba, "Efficiency enhancement in a light-emitting diode with a two-dimensional surface grating photonic crystal," *Appl. Phys. Lett.* **84**(4), 457–459 (2004).
5. J. W. Pan, S. H. Tu, W. S. Sun, C. M. Wang, and J. Y. Chang, "Integration of non-Lambertian LED and reflective optical element as efficient street lamp," *Opt. Express* **18**(S2 Suppl 2), A221–A230 (2010).
6. J. J. Chen, Y. K. Su, C. L. Lin, S. M. Chen, W. L. Li, and C. C. Kao, "Enhanced output power of GaN-based LEDs with nano-patterned sapphire substrates," *IEEE Photon. Technol. Lett.* **20**(13), 1193–1195 (2008).
7. Y. J. Lee, H. C. Kuo, T. C. Lu, B. J. Su, and S. C. Wang, "Fabrication and characterization of GaN-based LEDs grown on chemical wet-etched patterned sapphire substrates," *J. Electrochem. Soc.* **153**(12), G1106–G1111 (2006).
8. R. H. Horng, W. K. Wang, S. C. Huang, S. Y. Huang, S. H. Lin, C. F. Lin, and D. S. Wu, "Growth and characterization of 380-nm InGaN/AlGaIn LEDs grown on patterned sapphire substrates," *J. Cryst. Growth* **298**, 219–222 (2007).
9. J. K. Sheu, K. H. Chang, S. J. Tu, M. L. Lee, C. C. Yang, C. K. Hsu, and W. C. Lai, "InGaIn light-emitting diodes with oblique sidewall facets formed by selective growth on SiO<sub>2</sub> patterned GaN film," *Opt. Express* **18**(S4 Suppl 4), A562–A567 (2010).
10. S. J. Lee, "Analysis of light-emitting diodes by Monte Carlo photon simulation," *Appl. Opt.* **40**(9), 1427–1437 (2001).
11. T. X. Lee, C. Y. Lin, S. H. Ma, and C. C. Sun, "Analysis of position-dependent light extraction of GaN-based LEDs," *Opt. Express* **13**(11), 4175–4179 (2005).
12. W. K. Wang, D. S. Wu, S. H. Lin, S. Y. Huang, K. S. Wen, and R. H. Horng, "Growth and characterization of InGaIn-based light-emitting diodes on patterned sapphire substrates," *J. Phys. Chem. Solids* **69**(2-3), 714–718 (2008).
13. W. K. Wang, D. S. Wu, S. H. Lin, S. Y. Huang, P. Han, and R. H. Horng, "Characteristics of flip-chip InGaIn-based light-emitting diodes on patterned sapphire substrates," *Jpn. J. Appl. Phys.* **45**(4B), 3430–3432 (2006).
14. T. X. Lee, K. F. Gao, W. T. Chien, and C. C. Sun, "Light extraction analysis of GaN-based light-emitting diodes with surface texture and/or patterned substrate," *Opt. Express* **15**(11), 6670–6676 (2007).

15. C. C. Sun, C. Y. Lin, T. X. Lee, and T. H. Yang, "Enhancement of light extraction of GaN-based light-emitting diodes with a microstructure array," *Opt. Eng.* **43**(8), 1700–1701 (2004).
16. J. F. Muth, J. D. Brown, M. A. L. Johnson, Z. Yu, R. M. Kolbas, J. W. Cook, Jr., and J. F. Schetzina, "Absorption coefficient and refractive index of GaN, AlN and AlGaIn alloys," *MRS Internet J. Nitride Semicond. Res.* **4S1**, G5.2 (1999).
17. A. B. Djurić, Y. Chan, and B. H. Li, "Calculations of the refractive index of AlGaIn/GaN quantum well," *Proc. SPIE* **4283**, 630–637 (2001).
18. X. H. Wang, W. Y. Fu, P. T. Lai, and H. W. Choi, "Evaluation of InGaIn/GaN light-emitting diodes of circular geometry," *Opt. Express* **17**(25), 22311–22319 (2009).

## 1. Introduction

Light emitting diodes (LEDs) have come to be regarded as an important light source in recent years due to their many advantages such as energy saving, high reliability, longer lifetime, environmental protection, faster switching and compact forms. LEDs have gradually replaced traditional light sources such in display backlight units [1], traffic signals, automotive lighting, architectural lighting and aviation lighting. Currently, high power gallium-nitride (GaN)-based LED chips with phosphors are being adopted as white-light light sources for general lighting. However, improvements to the external quantum efficiency (EQE) are required especially in high power devices. The external quantum efficiency equals the multiplication of the internal quantum efficiency (IQE) and the light extraction efficiency (LEE). In recent years, the IQE of GaN-based LEDs has greatly improved due to use of good quality crystals, however the LEE is still low because of the large refractive index difference between the semiconductor and the surrounding medium. Approximately 4% of internal light can be extracted from the conventional GaN-based LED surface and the light escape cone is about 23 degrees [2]. Improving the LEE is important, and various methods such as surface textures [3–5], patterned sapphire substrates [6–8], chip shaping [9], and photonic crystals have been tested as a means to accomplish this.

Both wave and geometrical optics have been used to simulation the LEE of the LEDs. In geometrical optics, the rays with a uniform direction can be interrupted by various events, such as scattering, absorption and reemission in the active region, absorption inside the other semiconductor layers, or Fresnel loss of media with different refractive indices. The Monte Carlo ray tracing method has been applied in many studies of the LED chip because of the randomness of the photon emission from the active layer [10–14]. However, the relationship between the ray paths and LEE has not been adequately explained by the numerical data.

In this work, we study three types of GaN-based LEDs differing based on the different location of the pyramid textures. In case 1, the pyramid texture is located on the sapphire top surface, in case 2, the pyramid texture is located on the P-GaN top surface and in case 3, the pyramid textures are located on both the sapphire and P-GaN top surfaces. The relationship between the LEE and angle of slant of the pyramid texture is studied [15]. In all cases the pyramid texture has a width of  $5\mu\text{m}$  and a period of  $5\mu\text{m}$ . The optimal LEE is highest in case 3 among the three cases [11]. In addition, case 3 has a higher tolerance of slant angle than for cases 1 or 2. Moreover, the seven escape paths along which the most escaped photon flux propagates are also selected in an LED simulation. Since the seven escape paths occupy the largest part of the LEE, they dominate the LEE phenomenon in the LED and the paths can be explained by the angular space directly.

## 2. Optical structure and the theory of the escape cone

### 2.1 Optical structure of GaN-based LED chips

To introduce the GaN-based LEDs, Fig. 1 shows a schematic diagram of the GaN-based LED without the pyramid texture. The chip size was  $300 \times 300\mu\text{m}^2$  and the absorption coefficient of the active layer was assumed to be  $1\mu\text{m}^{-1}$  [16,17]. The structural parameters of the GaN-based LEDs are given in Table 1. The reflectivity of the sapphire bottom surface was 90%.



Fig. 1. Schematic diagram of the GaN-based LED without the pyramid texture.

**Table 1. Parameters of each layer in the simulated LED**

Chip size: $300 \times 300 \mu\text{m}^2$			
	Thickness( $\mu\text{m}$ )	Refractive Index	Absorption( $\mu\text{m}^{-1}$ )
<b>P-GaN</b>	0.05	2.45	0
<b>MQW</b>	0.1	2.54	1
<b>N-GaN</b>	2	2.42	0
<b>AlGaIn</b>	0.05	2.4	0
<b>GaN</b>	2	2.4	0
<b>Sapphire</b>	330	1.78	0

## 2.2 Theory of the escape cone in angular space

The total internal reflection is the main issue related to the trapping of light in the GaN-based LED chip. According to Snell's law, the critical angle  $R_1$  of the interface between the P-GaN layer and the air can be derived as in Eq. (1), where  $n_{\text{air}}$  is the refractive index of the air and  $n_{\text{P-GaN}}$  is the refractive index of the P-GaN layer.

$$\sin^{-1}(n_{\text{air}}/n_{\text{P-GaN}}) = R_1 \quad (1)$$

When the incidence angle of the photons emitted from the MQW is smaller than the critical  $R_1$ , the rays will no longer be trapped in the P-GaN layer. Because the incident angle determines whether the photons escape or not, we adopt the concept of the angular space to explain the LEE of the LED chip in the different cases. We also call this critical angle the escape cone for escaping light to form.

In Table 1, because the thicknesses of the P-GaN, MQW, N-GaN, AlGaIn and GaN layers are very small, the photons that escape from the four side surfaces of these layers can be ignored. Moreover, because the indices of these layers are similar, the internal total reflection and Fresnel loss can be ignored. In order to simplify the theory, we discuss only the five surfaces: the P-GaN top surface and the four sapphire side surfaces for photon escape. The P-GaN, MQW, N-GaN, AlGaIn and GaN layers are regarded as one layer with an index of 2.45 [18].

The Monte carol ray tracing software of LightTools is used to model phenomena of the geometrical optics. In the figures below we can see the results of the calculation obtained by Snell's law for ray tracing.

## 2.3 Photons emission toward the top

In the condition without any texture, the emission photons are divided into two types after the propagating from the P-GaN layer to the top, escaping and trapped photons. The two paths are labeled path A and path B as shown in Fig. 2(a) and 2(b).

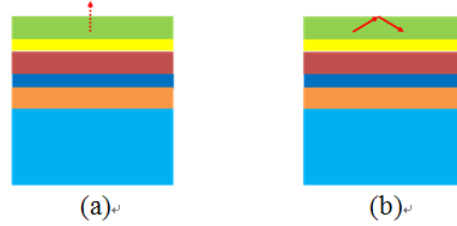


Fig. 2. Schematic diagrams of (a) path A and (b) path B.

Figures 3(a) and 3(b) show the distribution of the two types of emission in the angular space. The distribution in these figures is labeled region A and region B, respectively, which are complementary regions in the angular space. In Fig. 3(a), region A is a circle with a radius  $R_1$  of 24.09 degrees as obtained from Eq. (1). Moreover, the distribution is changed by applying the textures on the P-GaN top surface. For example, there is a change in region A from Fig. 3(a) to Fig. 3(c) obtained by applying the pyramid texture with a slant angle of 20 degrees on the P-GaN top surface. In Fig. 3(c), the four circles present the escape cone of the four slanted surfaces. Because the slant angle of the pyramid texture is 20 degrees, the center of the four circles is at a distance of 20 degrees from the origin of the angular space. The probability of escape of the photons increases with the increased density of the blue spots in Fig. 3(c).

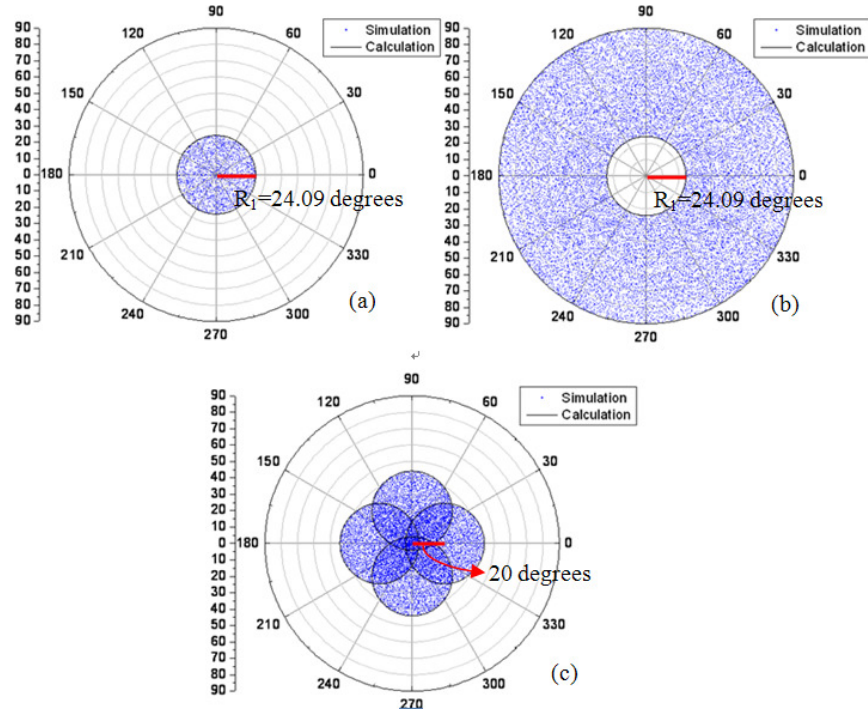


Fig. 3. (a) Region A without texture, (b) region B without the texture and (c) region A with a pyramid texture that has a slant angle of 20 degrees in the angular space.

#### 2.4 Photon emission toward the bottom

In the condition without any texture, the emitted photons are divided into three types after propagating from the P-GaN layer to the bottom. The three types are escaping photons, trapped photons resulting from being trapped by the reflective layer and trapped photons resulting from the total internal reflection created by the interface between the sapphire layer

and the GaN layer. The three paths are labeled path C, path D and path E as shown in Fig. 4(a), 4(b) and 4(c).

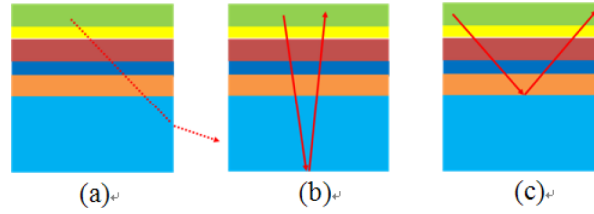


Fig. 4. Schematic diagrams of (a) path C, (b) D and (c) E.

Figures 5(a), 5(b) and 5(c) respectively explain the distribution of the three types of emission in angular space. The distribution is labeled by region C, region D and region E respectively which are complementary regions in angular space. In Fig. 5(a) the circle consists of region C and region D and has a radius  $R_2$  of 46.60 degrees. The radius  $R_2$  is obtained with Eq. (2). The  $n_{\text{sapphire}}$  is the refractive index of the sapphire layer.

$$\sin^{-1}(n_{\text{sapphire}}/n_{\text{P-GaN}}) = R_2 \quad (2)$$

The sapphire has four side surfaces, so that region C is distributed near the four side edges in the circle in Fig. 5(a). Moreover, the regions can be changed by applying textures to the top surface of the sapphire. For example, there is a change in region C from Fig. 5(a) to Fig. 5(d), caused by the pyramid texture with a slant angle of 30 degrees that formed on the top surface of the sapphire. There is a shift in the escape cones in four directions caused by the four slanted surfaces of the pyramid texture.

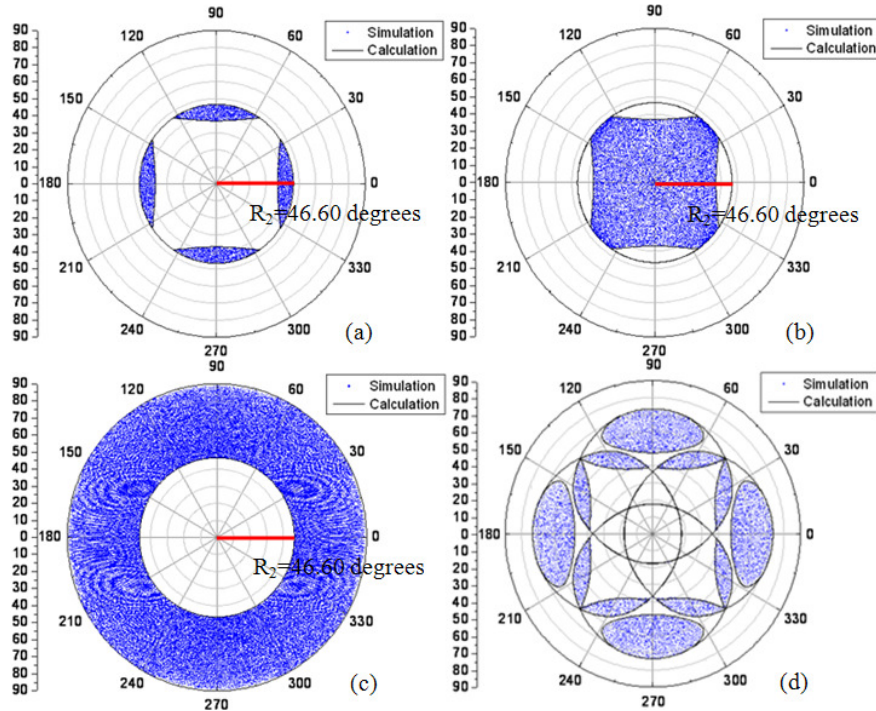


Fig. 5. (a) Region C without the texture, (b) region D without the texture, (c) region E without the texture and (d) region C with the texture with a slant angle of 20 degrees in the angular space.

### 3. LEE analysis using the ray path and angular space

In LED efficiency enhancement studies, a common way to enhance the LEE of the GaN-based is the processes of applying a texture on the P-GaN layer or the sapphire layer. We study three cases where GaN-based LEDs are classified based on the different locations of the pyramid textures. In case 1, the pyramid texture is located on the sapphire's top surface. In case 2, the pyramid texture is located on the P-GaN top surface. In case 3, the pyramid textures are located on both the sapphire and P-GaN top surfaces. The three cases are illustrated in Fig. 6(a), 6(b) and 6(c).

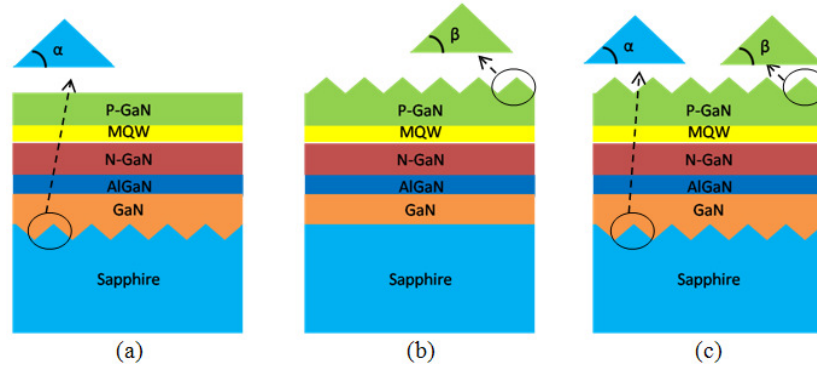


Fig. 6. Schematic diagram showing the three cases of GaN-based LEDs: (a) case 1, (b) case 2 and (c) case 3.

In order to analyze the relationship between the LEE and the slant angle of the pyramid texture in the three cases, seven photon escape paths are selected from the many ray paths for analysis, as shown in Fig. 7. The seven escape paths all originate from the LED. Because of the high probability of escape, the seven paths occupy a large part of the LEE and dominate the phenomenon of the LEE. Path 1 to path 5 all escape from the P-GaN top surface. Owing to the fact that the other paths have a low probability of escaping from the sapphire side surfaces, only path 6 and path 7 are selected. The seven escape paths are derived from paths A, B, C, D and E, therefore regions A, B, C, D and E are used to present the phenomenon of the angular space. The theory on which paths A to E and regions A to E are based is discussed in Section 2.

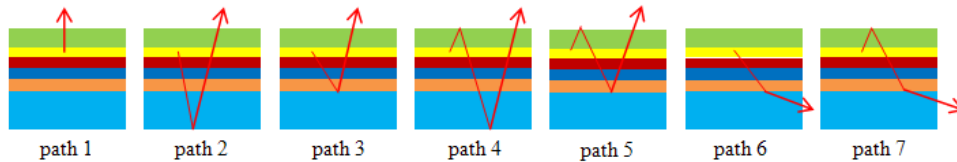


Fig. 7. Schematic diagrams of the seven escape paths.

#### 3.1 Case 1: Pyramid textures located on the sapphire's top surface

In case 1, the pyramid texture is applied to the sapphire's top surface. The slant angle of the pyramid texture is labeled  $\alpha$ , as shown in Fig. 6(a). Figure 8 shows the relationship between the total LEE for case 1 and  $\alpha$ . The optimized total LEE is 15.35% for an  $\alpha$  of 32 degrees. Since the range from 21 degrees to 42 degrees includes the optimization results, we calibrate the partial LEE in this range. The range is indicated by the red dashed lines in Fig. 8. Figure 9 in page 8 shows the relationship between the partial LEE of the seven escape paths and  $\alpha$ . The summation of the partial LEE of the seven escape paths has the optimal result for an  $\alpha$  of 32 degrees. Moreover, the optimized result for the total LEE for case 1 and the summation of the partial LEE for the seven escape paths for case 1 are consistent. Thus, the partial LEE analysis can be used to precisely analyze the photon escape path.



The partial LEE through different paths can be explained by the region of angular space, so we use the interaction between region A, B, C, D and E to explain the phenomenon of the partial LEE of the seven escape paths. Since there is no interaction between the pyramid textures along path 1, the partial LEE is not affected by the increased slant angle  $\alpha$ . Owing to the decrease in overlap region D of the four slanted surfaces due to the increased slanted angle  $\alpha$ , the probability decreased for path 2. The partial LEE decreased for path 2 with the decreased probability. For path 3, the increased overlap between region A and region E increased the probability of reflectivity. However, the distributions in regions C and D are enlarged by increases in  $\alpha$ , so that the probability of total internal reflection from the interface between the GaN layer and the sapphire layer of path 3 is decreased by the increased slant angle  $\alpha$ . Since the two factors constrain each other, the partial LEE of path 3 reaches its maximum value at an angle  $\alpha$  of 32 degrees. Path 4 could be divided into two sub-paths. In the first sub-path, the photons hit the P-GaN top surface and are total internal reflected toward the reflective layer. The first sub-path has the greater probability due to the increased overlap between region B and region D. Along the second sub-path, the photons are reflected from the reflective layer and escape from the P-GaN top surface. The second sub-path has a higher probability when increasing the overlap between region A and region D. Since the two factors constrain each other, the partial LEE of path 4 reaches its maximum value at an angle  $\alpha$  of 32 degrees. For path 5, we divide the path into two sub-paths. On the first sub-path, the photons are total internal reflected from the P-GaN top surface and there is total internal reflected from the interface between the P-GaN layer and the sapphire layer. The first sub-path has a greater probability by increasing the overlap between region B and region E. For the second sub-path, the photons are total internal reflected from the interface between the GaN layer and the sapphire layer and escape from the P-GaN top surface. The second step has a higher probability with increased overlap between region A and region E. Since the two factors constrain each other, the partial LEE of path 5 reaches its maximum value with an angle  $\alpha$  of 32 degrees and the partial LEE is zero until region A overlaps region E. For path 6, owing to the increased interaction area of the pyramid texture and the increased distribution of region C due to the increased  $\alpha$ , there is an increase in the partial LEE. For path 7, because of the increase in the overlap between region B and region C due to the increased  $\alpha$ , there is an increase in the partial LEE. However, the length of path 7 is increased by the increased angle  $\alpha$ , so there is a slight decrease in the partial LEE after  $\alpha$  reaches 36 degrees.

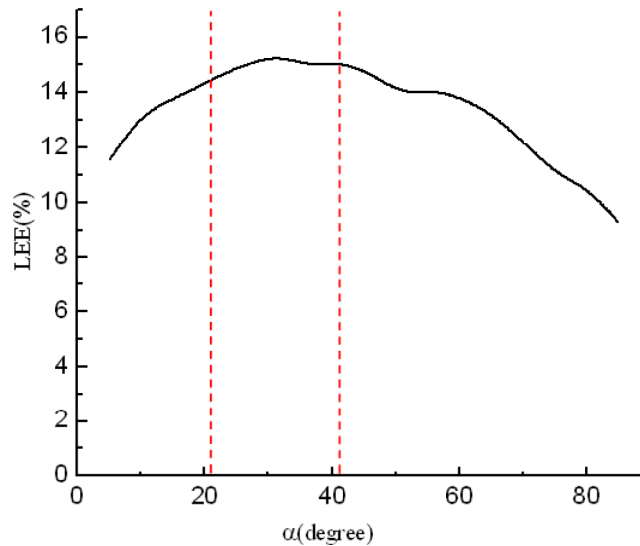


Fig. 8. Relationship between the total LEE for case 1 and  $\alpha$ .

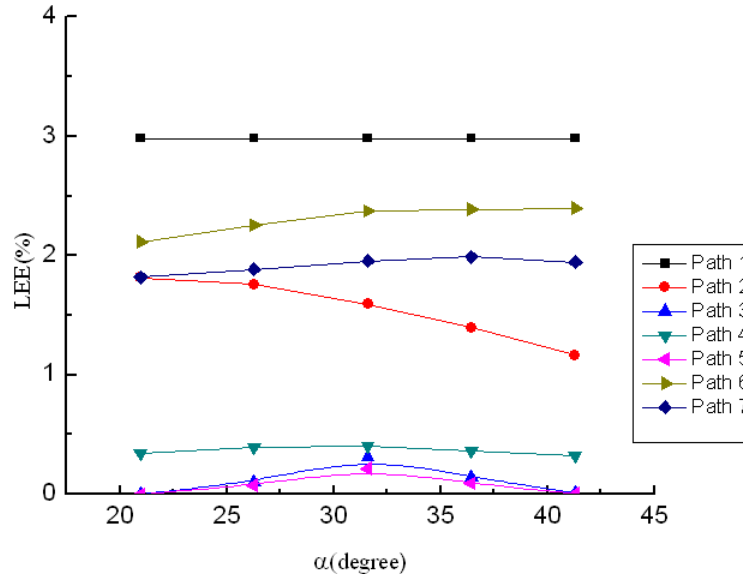


Fig. 9. Relationship between the partial LEE of the seven escape paths and  $\alpha$ .

### 3.2 Case 2: Pyramid texture located on the P-GaN top surface

In case 2, the pyramid texture was applied to the P-GaN top surface. The slant angle of the pyramid texture is labeled  $\beta$  as shown in Fig. 6(b). Figure 10 shows the relationship between the total LEE for case 2 and  $\beta$ . The optimal the total LEE was 15.83% for a  $\beta$  of 22 degrees [11]. The range from 16 degrees to 51 degrees includes the optimal result and localized minimum. Thus we calibrate the partial LEE in this range as shown by the dashed lines in Fig. 10. Figure 11 shows the relationship between the partial LEE of the seven escape paths and  $\beta$ . The summation of the partial LEE of the seven paths has an optimized result at a  $\beta$  of 22 degrees. Moreover, the optimization results for the total LEE for case 2 and the sum of the partial LEE from the seven escape paths for case 2 are consistent. Thus, partial LEE analysis can be used to precisely analyze the photon escape path.

For path 1, owing to the increased interaction area of the pyramid texture and the increased distribution of region A due to the increased  $\beta$ , there is an increase in the partial LEE. For path 2, because the overlap between regions A and D is decreased by the increased angle  $\beta$ , the partial LEE is decreased. For path 3, since there is an increase in the region of overlap between regions A and E by increase in  $\beta$ , there is an increase in the probability of the partial LEE being enlarged. Path 4 can be divided into two sub-paths. Along the first sub-path, the photons hit the P-GaN top surface and are total internal reflected toward the reflective layer. The first sub-path has a higher escape probability resulting from the increased overlap between regions B and D. On the second sub-path the photons are reflected from the reflective layer and escape from the P-GaN top surface. The second sub-path has the higher escape probability resulting from increasing overlap between region A and region D. Since the two factors constrain each other, the partial LEE of path 4 has its maximum value with an angle  $\beta$  of 27.5 degrees. Path 5 can be divided into two sub-paths. Along the first sub-path, the photons are total internal reflected from the P-GaN top surface and there is total internal reflectance from the interface between the GaN layer and the sapphire layer. The first sub-path has a greater probability with an increase in the overlap between regions B and E. In the second sub-step, the photons are total internal reflected from the interface between the GaN layer and the sapphire layer and escape from the P-GaN top surface. The second sub-path has a higher probability when the overlap between region A and region E increases. Since the two factors constrain each other, the partial LEE of path 5 reaches its maximum value at an angle  $\beta$  of 42 degrees and the partial LEE is zero until region A overlaps region E. For path 6, there



is no interaction with the pyramid texture, so the partial LEE is not affected by the increase in angle  $\beta$ . For path 7, since the overlap between regions B and C is decreased by the increased angle  $\beta$ , there is a decrease in the partial LEE with the increasing angle  $\beta$ .

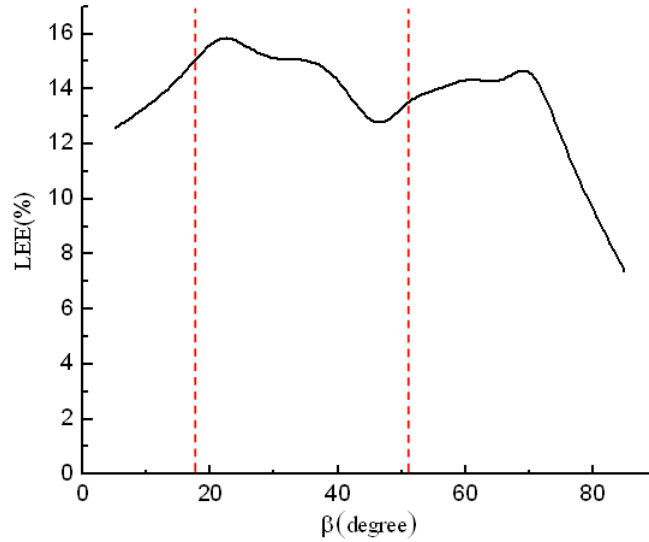


Fig. 10. Relationship between the total LEE for case 2 and  $\beta$ .

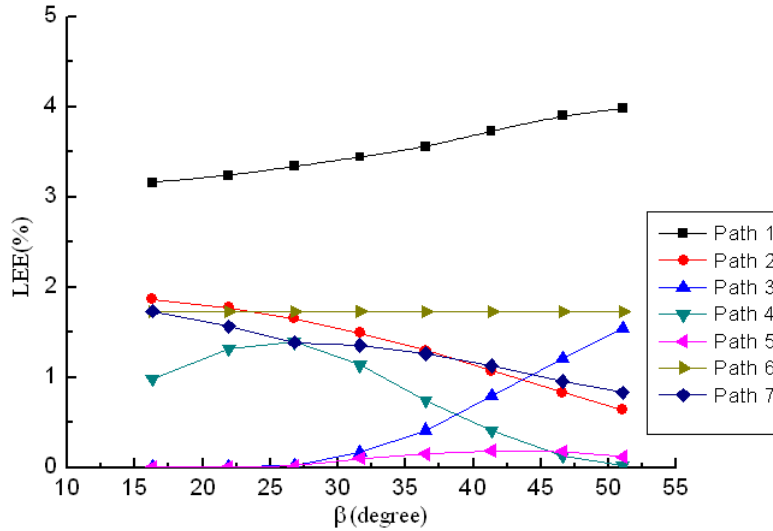


Fig. 11. Relationship between the partial LEE of the seven escape paths and  $\beta$ .

### 3.3 Case 3: Pyramid textures located on the P-GaN and sapphire top surfaces

In case 3, the pyramid texture was applied to the sapphire top surface and the P-GaN top surface. The slant angle of the pyramid texture on the sapphire top surface is labeled  $\alpha$  and the slant angle of the pyramid texture on the P-GaN top surface is labeled  $\beta$ , as shown in the Fig. 6(c). Figure 12 shows the relationship between the total LEE for case 3,  $\alpha$  and  $\beta$ . The optimized total LEE is 17.72% at an  $\alpha$  of 43 degrees and  $\beta$  of 25 degrees. Moreover, the summation of the partial LEE of the seven escape paths has an optimized result at an  $\alpha$  of 43 degrees and  $\beta$  of 25 degrees. The optimal result of the total LEE for case 3 and the summation

of the partial LEE for the seven escape paths for case 3 are consistent. Thus, partial LEE analysis can be used to precisely analyze the photon escape paths.

In the optimization results for the three cases, the optimized LEE of case 3 is better than for the previous two cases. Moreover, the higher texture density in the GaN-based LED enhances the scattering effect, so the total LEE is uniform throughout a larger angular region. Thanks to the smaller variation of the total LEE, case 3 has a higher tolerance of slant angle than for case 1 and case 2. The seven escape paths could also be explained by the angular space, as discussed in section 3.1 and 3.2.

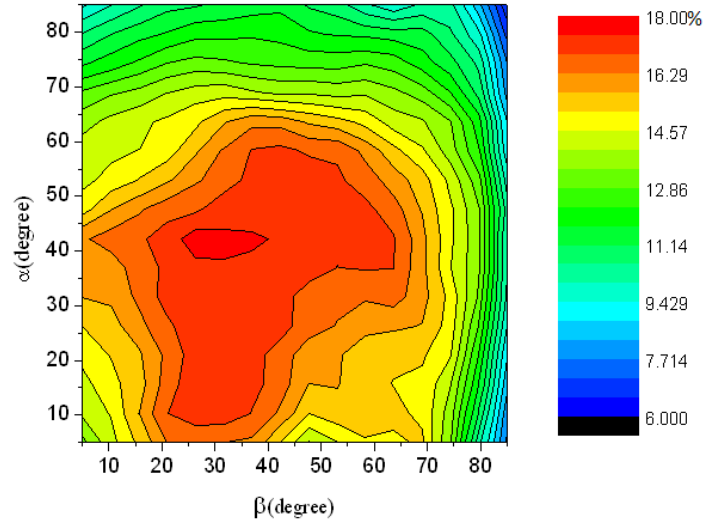


Fig. 12. Relationship between the total LEE for case 3,  $\alpha$  and  $\beta$ .

**Table 2. Optimization results for the three cases**

Type	Conventional	Case 1	Case 2	Case 3
Total LEE (%)	9.04	15.35	15.83	17.72
Slant angle of the pyramid texture (degrees)		$\alpha = 32$	$\beta = 22$	$\alpha = 43$ $\beta = 25$
LEE (%)	Path 1	2.95	2.95	3.25
	Path 2	1.75	1.57	1.77
	Path 3	0.00	0.31	0.00
	Path 4	0.00	0.38	1.42
	Path 5	0.00	0.21	0.00
	Path 6	1.72	2.35	1.72
	Path 7	1.50	1.91	1.56

We summarize and the optimization results for cases 1, 2 and 3 in Table 2. And the result of the conventional LED without any texture is listed to be the reference data in Table 2. The order of optimized total LEE for the three cases is as follows: case 3, case 2 and case 1 [11]. The order of the summation of the partial LEE for paths 1 to 7 is consistent with the optimized total LEE results. Thus, partial LEE analysis can be used to analyze the photon escape path quite precisely. When the texture is only introduced on a single interface, case 2 is a better choice due to the higher total LEE. In case 1, because the summation of the partial LEE of paths 6 and 7 is highest among the three cases, case 1 has a higher ability to enlarge the photon flux that escapes from the four sapphire side surfaces. In case 2, because the summation of the partial LEE of paths 1 to 5 is highest among the three cases, this case has a higher ability to enlarge the photon flux that escapes from the P-GaN top surface. Case 3 is a combination of structures for case 1 and case 2. However, the parameters  $\alpha$  and  $\beta$  are different. The overlap between region A and region C means that a part of the photons that

escape from the P-GaN top surface become photons that escape from the four sapphire side surfaces. In other words, the overlap between regions A and C reduces the utilization efficiency of the overall photons that are emitted from the MQW.

#### **4. Conclusion**

In this paper, we study three types of the GaN-based LED based on the different locations of the pyramid textures. In case 1, the pyramid texture was located on the sapphire top surface. In case 2, the pyramid texture was located on the P-GaN top surface. In case 3, the pyramid texture was located on both surfaces. We adopted the angular space region to explain the LEE of the LED chip under different conditions. The seven escape paths that dominate the phenomena of the LEE in the LED are used to analyze the relation between the geometric parameters of the texture and the LEE of the LED. The optimized total LEE is highest for case 3. The total LEE for this case is not sensitive to changes in the slant angle of both the top and bottom surface textures. Because the higher texture density in the GaN-based LED enhances the scattering effect, the total LEE is uniform throughout a larger angular region. In addition, the ability to enlarge the photon flux escaping from the four sapphire side surfaces is greater in case 2 and the ability to enlarge the photon flux escaping from the P-GaN top surface is greater in case 3. Moreover, the summarization of the partial LEE resulting from the seven escape paths is consistent with the total LEE, meaning that the partial LEE method can be used to analyze the escape photon behavior in detail and estimate the optimization angle precisely.

#### **Acknowledgment**

This study was supported in part by the National Science Council, project numbers NSC100-2220-E-009-023, NSC101-2314-B-384-001, and NSC101-2220-E-009-021, in part by the “Aim for the Top University Plan” of the National Chiao Tung University and the Ministry of Education, Taiwan. The optical simulation LightTools software was supported by CYBERNET SYSTEMS TAIWAN under the Synopsys education license agreement.